

Three-dimensional volumetric assessment of coronary artery calcification in patients with stable coronary artery disease by OCT



Parasuram Krishnamoorthy¹, MD; Yuliya Vengrenyuk², PhD; Hiroshi Ueda², MD; Takahiro Yoshimura², MD; Jacobo Pena², MD; Sadako Motoyama², MD, PhD; Usman Baber², MD; Choudhury Hasan², MD; Srinivas Kesanakurthy², MD; Joseph M. Sweeny², MD; Samin K. Sharma², MD; Jagat Narula², MD, PhD; Jason C. Kovacic², MD, PhD; Annapoorna S. Kini^{2*}, MD

1. Department of Cardiology, Albert Einstein Medical Center, Philadelphia, PA, USA; 2. Division of Cardiology, Icahn School of Medicine at Mount Sinai, New York, NY, USA

This paper also includes supplementary data published online at: http://www.pcronline.com/eurointervention/118th_issue/48

KEYWORDS

- coronary artery calcification
- diabetes mellitus
- lipid volume index
- optical coherence tomography
- plaque cap thickness

Abstract

Aims: There is a lack of a reliable technique to quantify coronary artery calcification (CAC). Hence, we used optical coherence tomography (OCT) to quantitate three-dimensional CAC volume to examine its association with plaque characteristics.

Methods and results: A total of 250 patients with stable angina undergoing OCT imaging before PCI were included. CAC volume was calculated from every frame of the culprit lesion and divided into tertiles (low, intermediate and high). Quantitative calcium characteristics were assessed in 107 patients who underwent both OCT and IVUS. Increase in CAC volume was associated with reduced lipid volume index, lipid length and number of lipid plaques. Diabetes and LDL cholesterol predicted less coronary calcification whereas age and prior MI predicted increased CAC after adjusting for all clinical factors. Lipid volume index ($\rho=-0.001$ [-0.003 to -0.00003]; $p=0.04$) and mean calcium depth ($\rho=-0.02$ [-0.02 to -0.01]; $p=0.000$) were inversely related to CAC volume after adjusting for all OCT characteristics, whereas cap thickness increased with increase in CAC volume ($\rho=0.01$ [0.002-0.03]; $p=0.02$) only in unadjusted analysis. Regression analysis demonstrated a significant correlation between calcium length ($\rho=0.83$; $p<0.001$) and calcium arc ($\rho=0.86$; $p<0.001$) measured by IVUS and OCT.

Conclusions: Target lesions with high CAC volume are characterised by reduced plaque lipid content and calcium closer to the luminal border. Fibrous cap thickness increased with increase in calcium volume.

*Corresponding author: Mount Sinai Hospital, One Gustave L Levy Place, Box 1030, New York, NY 10029, USA.
E-mail: annapoorna.kini@mountsinai.org

Abbreviations

ACS	acute coronary syndrome
ANOVA	one-way analysis of variance
CAC	coronary artery calcification
CSA	cross-sectional area
IVUS	intravascular ultrasound
OCT	optical coherence tomography
PCI	percutaneous coronary intervention
QCA	quantitative coronary angiography
TCFA	thin-cap fibroatheroma

Introduction

Despite advances in diagnosis and management, acute coronary syndrome (ACS) still remains the leading cause of mortality and morbidity in the USA and worldwide¹. Our understanding of the pathophysiology of ACS has evolved tremendously and involves a delicate balance between endothelial dysfunction, thrombogenicity of the blood and activation of inflammatory biomarkers through different cascades². Acute thrombosis and plaque rupture remain the most common reasons for sudden cardiac death and acute myocardial infarction³. Although the progression of an atherosclerotic lesion is unpredictable, certain morphological features including fibrous cap thickness of atheroma, necrotic core size and degree of inflammation play a key role in determining plaque stability and rendering the plaque vulnerable⁴. Coronary artery calcification (CAC) is a feature of advanced atherosclerosis⁵. Its clinical implications in and around the region of an atheroma are still unclear⁶. It may influence biomechanical stress and plaque stability when present close to or within the lesion⁷. The fact that there are no reliable techniques to quantify the extent of CAC *in vivo* poses an additional challenge to the study of the relationship between coronary calcification and plaque morphology. Intravascular ultrasound (IVUS) has been used to study CAC⁸ and differing patterns of calcification in ACS, namely ST-segment elevation myocardial infarction (STEMI), non-ST-segment elevation myocardial infarction (NSTEMI) and unstable angina⁹, but has limited ability due to poor spatial resolution and high reflection. Kataoka et al analysed the relation between spotty calcification and plaque vulnerability *in vivo* using optical coherence tomography (OCT)¹⁰. However, volumetric analysis of CAC, a more accurate measure of coronary calcium, has not been performed using OCT. Hence, in this study we used OCT to estimate the three-dimensional CAC volume *in vivo* to examine the association of CAC volume with plaque characteristics and clinical profile.

Methods

STUDY POPULATION

We performed a retrospective analysis of prospectively collected data of 250 consecutive patients from the institutional review board-approved clinical and imaging database with stable coronary artery disease (CAD) referred to the Mount Sinai Cardiac catheterisation lab from 2012 to 2014 and who also underwent OCT imaging prior to percutaneous coronary intervention (PCI). All lesions represented *de novo* atherosclerosis. Analysis was restricted to the target vessel.

Patients with renal failure (serum creatinine >1.5 mg/dl), haemodynamic compromise, contrast allergy, and aorto-ostial coronary artery lesions were excluded. Subset analysis comparing CAC assessments within the same lesion was performed in patients who underwent both OCT and IVUS examination (n=107).

OCT IMAGE ACQUISITION

OCT image acquisition was performed with a commercially available OCT intravascular imaging system (C7 Dragonfly™; St. Jude Medical, St. Paul, MN, USA). The catheter was placed at least 10 mm distally to the imaging target lesion with continuous intracoronary contrast injection (Visipaque™; GE Healthcare, Chicago, IL, USA), total volume 12-16 ml injected at 3-4 ml/sec) and simultaneous OCT catheter pullback at 20 mm/s.

OCT IMAGE ANALYSIS

Images were analysed at 1 mm intervals as validated before using the St. Jude Medical Offline Review Workstation¹¹⁻¹³. The smallest cross-sectional area (CSA), reference CSA, and percent lumen area stenosis were calculated for each lesion. OCT reference lumen CSA was estimated as the average value of proximal and distal references defined as the largest lumen proximal or distal to a stenosis but within the same segment. Lipid arc was measured at 1 mm intervals through the entire length of the lesion and lipid length was measured on longitudinal view. Lipid volume index was calculated as the averaged lipid arc multiplied by lipid length¹⁴. Fibrous cap thickness was estimated by measuring the thinnest signal-rich zone separating the lipid content from the vessel lumen in the entire stenosis. OCT thin-cap fibroatheroma (OCT-TCFA) was defined as a plaque with lipid arc >90° and fibrous cap thickness <65 µm. Plaque rupture was defined as the presence of discontinuity in the fibrous cap leading to a communication between the inner (necrotic) core of the plaque and the lumen^{11,15}. Three different OCT analysts reviewed OCT pullbacks independently at intervals of at least two weeks by the first observer to assess for interobserver variability.

CALCIUM ANALYSIS

Each frame of the OCT images was analysed for coronary calcification as previously validated^{16,17} using the St. Jude Medical Offline Review Workstation. Areas with poor signal and well-defined borders were classified as calcified plaques. The degree of circumferential extent of calcification was quantified, and average and maximal calcification arc was calculated for each lesion. Calcification length was calculated by multiplying the number of consecutive cross-sections containing calcification by slice thickness. Calcium depth was defined as the minimal distance between the luminal border of the calcific plaque and the lumen contour; mean and minimal calcium-lumen distance was calculated for each calcification. Calcium volume was calculated by Simpson's rule and by area measurements from every single frame (**Figure 1**). Calcified plaques seen by OCT were separated into two groups according to the ability to identify the abluminal

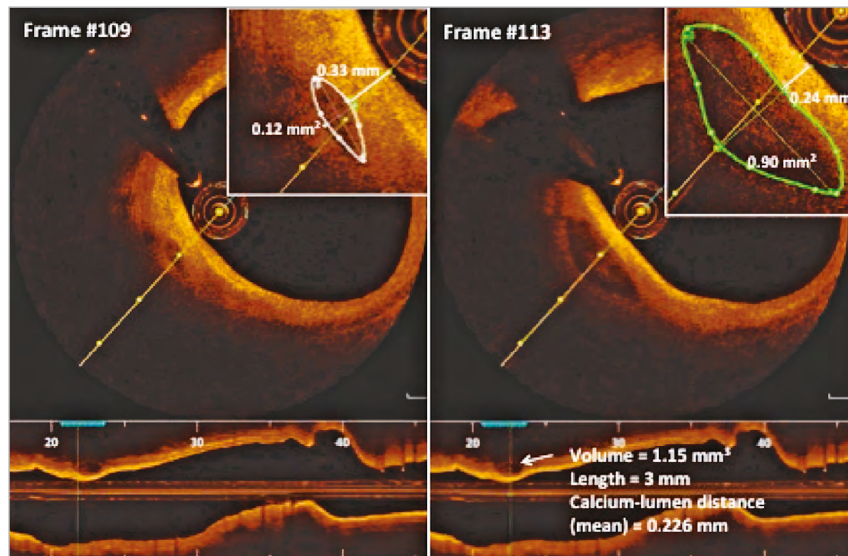


Figure 1. Volumetric characterisation of human coronary calcium in different frames by optical coherence tomography.

calcium border (group A) (**Figure 2**) or requirement to interpolate tracings in cases where the abluminal border was not visualised (group B) (**Figure 3**). An independent observer performed CAC volume assessment in 50 OCT pullbacks to assess reproducibility.

IVUS IMAGE ANALYSIS

Quantitative greyscale IVUS analysis was performed using QIvus 3.0 (Medis, Leiden, the Netherlands) according to the ACC consensus statement¹⁸ and as previously described^{12,13} to estimate

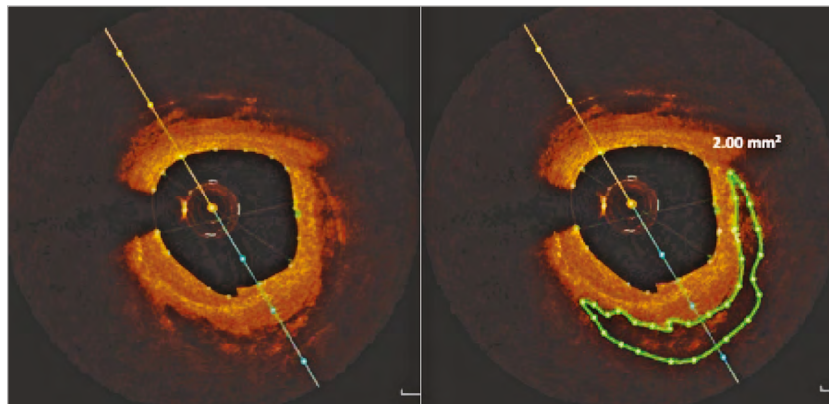


Figure 2. Volumetric assessment of group A calcium.

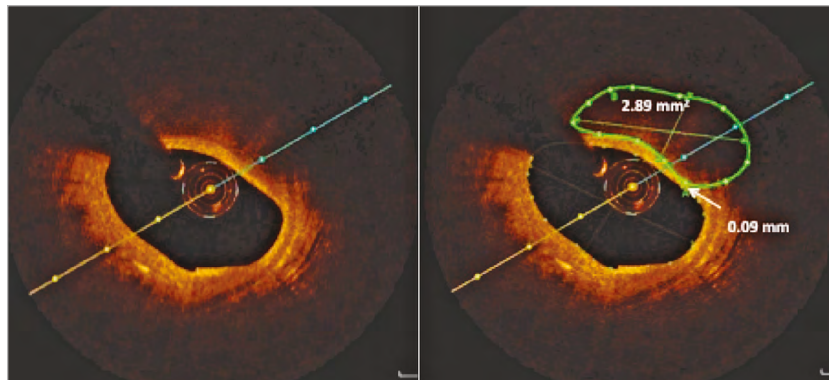


Figure 3. Volumetric assessment of group B calcium where tracing interpolation is required.

lumen and reference CSA, external elastic membrane (EEM) CSA, plaque plus media CSA, plaque burden, and the remodelling index (lesion EEM CSA/reference EEM CSA).

STATISTICAL ANALYSIS

Continuous measurements were reported as mean±SD if normally distributed and median (interquartile range) for non-parametric variables. One-way analysis of variance (ANOVA) and the Kruskal-Wallis test were used for comparing parametric and non-parametric continuous measurements. Categorical variables were expressed as frequency (percentages) and the chi-square test was used to compare between the calcium tertiles. Unadjusted and multivariable adjusted linear regression analysis was performed to examine the independent predictors of CAC. Bland-Altman analysis and regression analysis were performed to compare the mean differences (bias) and standard deviation between OCT and IVUS-defined maximal calcium arc and length¹⁹. Interobserver agreement and intraobserver reproducibility of imaging parameter measurements were assessed by intraclass correlation coefficients (ICC) based on the random effects analysis of variance models²⁰. All statistical analysis was performed using Stata/SE 11.0 (StataCorp LP, College Station, TX, USA).

Results

PATIENT CHARACTERISTICS AND OCT IMAGE ANALYSIS

Table 1 shows the baseline clinical and OCT characteristics of the 250 patients included in this study. Target lesions were divided into tertiles according to CAC volume (low 0.01±0.04, intermediate 1.14±0.7, and high 7.1±5.4 mm³; p<0.0001). Other baseline angiographic and procedural characteristics are described in **Online Table 1**. A trend towards an increase in coronary calcification was seen with an increase in age (p=0.07) and in males (p=0.19). Diabetes (p=0.02) was low in prevalence with increase in CAC. Patients who had a prior history of MI (p=0.01) had significantly increased coronary calcification. No relationship was observed with body habitus, renal function and CAC. Increase in CAC volume was associated with a significant decrease in lipid content, including number of lipid plaques (p<0.01), maximum (p=0.01) and average lipid arcs (p=0.04), lipid volume index (p=0.001), and lipid length (p<0.001). However, there was no significant difference between lumen area, minimal cap thickness of atheroma and plaque rupture. The depth of the calcium from the luminal border decreased with increase in CAC volume (p=0.02). Eight percent (8%) of lesions (n=20) required interpolation, out of which only 28% of frames (number of frames=198) within these lesions were group B lesions. The mean values for the total calcium volume by observer 1 (P. Krishnamoorthy) and observer 2 (H. Ueda) were 2.95±5.76 mm³ and 2.93±5.99 mm³, respectively. Bland-Altman analysis demonstrated high agreement for the measurement: mean difference (standard deviation) was -0.019±0.66 mm³ (**Online Figure 1**). The intraclass correlation coefficient for interobserver and intraobserver variability for the maximum lipid arc was 0.98 (95% CI: 0.93-0.99) and 0.99 (95% CI: 0.96-0.99), respectively;

for fibrous cap thickness it was 0.96 (95% CI: 0.87-0.99) and 0.98 (95% CI: 0.93-0.99), respectively.

PREDICTORS OF CAC VOLUME

Table 2 describes the unadjusted linear regression of clinical factors and OCT characteristics with CAC volume as dependent outcome. Age (0.07 [0.001 to 0.13]), male gender (1.75 [0.21 to 3.27]) and prior MI (2.42 [0.23 to 4.60]) predicted increased coronary calcification whereas diabetes (-1.56 [-2.98 to -0.13]), total (-0.03 [-0.04 to -0.01]) and LDL cholesterol (-0.03 [-0.06 to -0.01]) predicted less CAC. Consistent with prior findings in **Table 1**, lipid content was inversely associated with coronary calcification including lipid volume index (-0.001 [-0.02 to -0.001]), number of lipid-rich plaques (-3.09 [-4.9 to -1.2]), maximum (-0.01 [-0.02 to -0.003]) and average lipid arcs (-0.02 [-0.03 to -0.01]) and lipid length (-0.26 [-0.40 to -0.12]). Increase in CAC volume was associated with an increase in minimal fibrous cap thickness of atheroma (0.01 [0.002 to 0.03]). Calcium depth from the luminal border decreased with increase in CAC volume. When adjusted for all confounding clinical factors in the multivariable linear regression (**Table 3A**), age (0.07 [0.01 to 0.14]) and prior history of MI (2.64 [0.44 to 4.84]) still predicted more CAC, while diabetes (-1.46 [-2.86 to -0.07]) and LDL cholesterol (-0.03 [-0.05 to -0.01]) were associated with less CAC. Among the OCT characteristics (**Table 3B**), depth of calcium (-0.02 [-0.02 to -0.01]) and lipid volume index (-0.001 [-0.003 to -0.00003]) remained independent predictors of the extent of CAC. When adjusted for both clinical and OCT factors in the same model, prior MI (4.1 [1.55 to 6.54]; p=0.02) and lipid volume index (-0.002 [-0.003 to 0.0001]; p=0.05) were still significantly associated with CAC (**Online Table 2**). **Online Table 3** shows multivariable regression analysis adjusted for both clinical and OCT characteristics when total calcium volume was analysed as a binary variable.

CAC ASSESSMENT BY OCT AND IVUS

In 107 patients who underwent both IVUS and OCT examination, there was no difference in the prevalence of calcified plaques detected by OCT (79; 74%) and IVUS (74; 69%) (p=0.61). The maximal arc of calcium was 108.1±82.2° by OCT and 103.8±85.0° by IVUS, while calcium length was 3.6±3.8 mm and IVUS 4.3±4.2 mm by OCT and IVUS, respectively. Regression analysis demonstrated a significant correlation between calcium length (ρ=0.83; p<0.001) and calcium arc (ρ=0.86; p<0.001) measured by IVUS and OCT, respectively. Bland-Altman plots of mean calcium arc and length by OCT and IVUS imaging did not show any significant difference (**Online Figure 2**, **Online Figure 3**). Correlation between CAC assessment by QCA and OCT is shown in **Online Figure 4A** and **4B**.

Discussion

We present the results from what we believe is the first study to assess three-dimensional volumetric CAC using OCT. Key findings include the following. 1) CAC volume was inversely

Table 1. Baseline clinical and OCT characteristics of the study population.

Variable*	Total N=250	Ca group 1 N=84	Ca group 2 N=83	Ca group 3 N=83	p-value [†]
Clinical characteristics					
Age, years	63.1±11	61.5±12	62.5±11	65.2±10	0.07
Male gender, n (%)	172 (69)	53 (63)	56 (67)	63 (76)	0.19
Body mass index, kg/m ²	28.3 (25.7-32.2)	27.9 (25.4-32.4)	28.5 (26.3-33.3)	27.9 (24.9-31.3)	0.34
Weight, kg	80 (70-91)	77 (69-92)	82 (73-92)	79 (70-91)	0.59
Height, cm	168.8±9.2	167.9±10	168.2±9	170.3±9	0.19
Body surface area, m ²	1.93 (1.79-2.11)	1.92 (1.77-2.14)	1.96 (1.83-2.09)	1.93 (1.79-2.12)	0.54
Diabetes, n (%)	130 (52)	54 (64)	38 (46)	38 (46)	0.02
Hypertension, n (%)	228 (91)	78 (93)	72 (87)	78 (94)	0.20
Dyslipidaemia, n (%)	207 (83)	70 (83)	69 (83)	68 (82)	0.96
Prior MI, n (%)	30 (12)	7 (8)	6 (7)	17 (20)	0.01
Prior CVA, n (%)	10 (5)	3 (5)	5 (7)	2 (3)	0.50
Statin use, n (%)	177 (71)	56 (67)	63 (76)	58 (71)	0.48
Current smoker, n (%)	59 (19)	22 (26)	21 (25)	16 (19)	0.52
Past smoker, n (%)	46 (14)	14 (17)	14 (17)	18 (22)	0.64
Insulin use, n (%)	31 (12)	14 (17)	9 (11)	8 (10)	0.33
Total cholesterol, mg/dl	141 (122-172)	146 (125-182)	141 (120-169)	137 (113-169)	0.22
HDL cholesterol, mg/dl	39 (33-48)	39 (32-46)	40 (33-47)	41 (35-49)	0.35
LDL cholesterol mg/dl	77 (58-102)	84 (64-106)	77 (54-104)	71 (55-99)	0.21
Triglyceride, mg/dl	102 (69-154)	119 (75-178)	106 (69-135)	98 (61-147)	0.11
Haemoglobin A1c	7 (6-8.5)	7.3 (6.1-9.5)	6.9 (6-8.3)	6.8 (6-8.6)	0.38
Cr Cl (Cockcroft-Gault)	84.6 (63.9-108)	81.9 (60.7-104)	84.9 (68.6-115)	84.5 (63.8-108)	0.89
Maximum troponin I leak	0 (0-0.2)	0 (0-0.2)	0 (0-0.2)	0 (0-0.1)	0.89
OCT characteristics					
Reference lumen CSA, mm ²	6.3 (4.8-7.7)	6.3 (4.9-7.9)	6.4 (4.7-8.2)	6.3 (4.7-7.5)	0.77
Minimum lumen CSA, mm ²	1.74 (1.2-2.7)	1.68 (1.2-2.6)	1.69 (1.2-2.4)	1.89 (1.3-2.9)	0.35
Lumen area stenosis	69.6 (59.6-78.2)	70.4 (59.6-70.4)	69.8 (63.2-80.6)	67.9 (51.7-77.9)	0.14
Lipid-rich plaques, n (%)	208 (83)	74 (88)	74 (89)	60 (72)	<0.01
Maximum lipid arc, °	175 (101-260)	182 (124-268)	188 (113-270)	120 (0-240)	0.01
Average lipid arc, °	110 (72-155)	121 (88-146)	112 (79-160)	93 (0-159)	0.04
Lipid length, µm	5 (2-10)	7 (2.5-10)	6 (2-11)	3.8 (0-7)	<0.001
Lipid volume index, ° x µm	620 (147-1,338)	851 (246-1,451)	646 (199-1,390)	350 (0-934)	0.001
TCFA, n (%)	56 (18)	21 (25)	14 (17)	21 (25)	0.33
Minimum cap thickness, µm	90 (60-120)	90 (60-120)	90 (70-120)	85 (60-125)	0.57
Plaque rupture, n (%)	25 (11)	8 (10)	7 (9)	10 (13)	0.69
Calcium total volume	1.02 (0-4.15)	0 (0-0)	1.03 (0.63-2)	7.23 (4.2-11.9)	0.0001
Calcium depth mean	128 (87-193)	190 (107-280)	143 (87-209)	118 (86-163)	0.02
Calcium depth minimum	30 (20-60)	140 (80-220)	50 (20-80)	20 (10-30)	0.0001

*Mean±SD for normally distributed continuous variables and median (IQR) for non-parametric variables; categorical variables expressed as n (%).
[†]ANOVA for normally distributed continuous variables and Kruskal-Wallis test for non-parametric variables; chi-square test for categorical variables.
 CSA: cross-sectional area; CVA: cardiovascular accident; HDL: high-density lipoprotein; LDL: low-density lipoprotein; MI: myocardial infarction;
 OCT: optical coherence tomography

associated with lipid volume in the plaque. 2) CAC volume was lower in diabetics. 3) Lesions with increased CAC were more likely to be closer to the vessel luminal border. 4) Increase in CAC was associated with increase in cap thickness although only in unadjusted analysis. 5) There was a strong correlation between coronary calcium measured by OCT when compared to IVUS imaging.

We demonstrated an inverse relationship between CAC and lipid volume present inside a plaque *in vivo*. Decrease in lipid plaque content by the use of statins could stimulate more macrophages, vascular smooth muscle cells and osteoclast-like cells, resulting in increased calcification by generating extracellular matrix²¹. This finding is also consistent with a recently published *post hoc* patient-level analysis of coronary calcium volume using

Table 2. Unadjusted linear regression of clinical factors and OCT characteristics with total calcium volume.

Variable	Partial regression coefficients	p-value
Clinical characteristics		
Age	0.07 [0.001 to 0.13]	0.04
Male gender	1.75 [0.21 to 3.27]	0.02
Body mass index	-0.05 [-0.15 to 0.06]	0.42
Weight	-0.004 [-0.03 to 0.02]	0.79
Height	0.04 [-0.03 to 0.11]	0.33
Body surface area	-0.19 [-3.01 to 2.62]	0.89
Diabetes	-1.56 [-2.98 to -0.13]	0.03
Hypertension	1.51 [-1.02 to 4.03]	0.24
Dyslipidaemia	-0.48 [-2.38 to 1.42]	0.62
Prior MI	2.42 [0.23 to 4.60]	0.03
Prior CVA	0.01 [-3.4 to 3.42]	0.99
Statin use	0.79 [0.81 to 2.38]	0.33
Smoker	-0.31 [-1.23 to 0.61]	0.50
Insulin use	-1.21 [-3.38 to 0.96]	0.27
Total cholesterol	-0.03 [-0.04 to -0.01]	0.005
HDL cholesterol	0.02 [-0.03 to 0.07]	0.54
LDL cholesterol	-0.03 [-0.06 to -0.01]	0.003
Triglyceride	-0.004 [-0.01 to 0.02]	0.16
Haemoglobin A1c	-0.14 [-0.51 to 0.22]	0.44
Cr Cl (Cockcroft-Gault)	-0.004 [-0.02 to 0.01]	0.66
Maximum troponin leak	-0.24 [-0.67 to 0.18]	0.26
OCT characteristics		
Reference lumen	-0.04 [-0.32 to 0.23]	0.76
Minimum lesion lumen	0.26 [-0.47 to 0.99]	0.48
Lumen area stenosis	-0.02 [-0.77 to 0.03]	0.43
Lipid-rich plaques	-3.09 [-4.9 to -1.2]	0.001
Maximum lipid arc	-0.01 [-0.02 to -0.003]	0.002
Average lipid arc	-0.02 [-0.03 to -0.01]	0.003
Lipid length	-0.26 [-0.40 to -0.12]	0.000
Lipid volume index	-0.001 [-0.02 to -0.001]	0.000
TCFA	-0.07 [-1.79 to 1.64]	0.93
Minimum cap thickness	0.01 [0.002 to 0.03]	0.02
Plaque rupture	0.93 [-1.22 to 3.1]	0.39
Calcium depth mean	-0.02 [-0.03 to -0.01]	0.000
Calcium depth minimum	-0.03 [-0.04 to -0.01]	0.000

CVA: cardiovascular accident; HDL: high-density lipoprotein; LDL: low-density lipoprotein; MI: myocardial infarction; OCT: optical coherence tomography; TCFA: thin-cap fibroatheroma

IVUS from eight different prospective RCTs where the use of statins was associated with an increase in coronary atheroma formation independent of their effects on plaque regression²². This could also potentially explain the results seen from prior studies that the use of statins was not effective in decreasing the CAC score as assessed by electron beam computed tomography (EBCT)^{23,24}.

Table 3A. Multivariable adjusted linear regression of clinical characteristics with total calcium volume.

Variable*	Partial regression coefficients	p-value
Age	0.07 [0.01 to 0.14]	0.02
Male gender	1.34 [-0.19 to 2.87]	0.08
Diabetes	-1.46 [-2.86 to -0.07]	0.04
Prior MI	2.64 [0.44 to 4.84]	0.01
LDL cholesterol	-0.03 [-0.05 to -0.01]	0.01

LDL: low-density lipoprotein; MI: myocardial infarction; OCT: optical coherence tomography

Table 3B. Multivariable adjusted linear regression of OCT characteristics with total calcium volume.

Variable*	Partial regression coefficients	p-value
Lipid volume index	-0.001 [-0.003 to -0.00003]	0.04
Average lipid arc	0.01 [-0.01 to 0.03]	0.34
Minimum cap thickness	0.01 [-0.01 to 0.03]	0.17
Calcium depth mean	-0.02 [-0.02 to -0.01]	0.000

*Model adjusted for all OCT characteristics that predicted calcium volume in unadjusted linear regression.

In our study, we observed that diabetes predicted less CAC volume in both univariate and multivariable regression analysis. This conflicts with previous findings and a common notion that increased CAC volume and progression of vascular calcification is commonly seen in diabetes²⁵ and is closely related to cardiovascular outcomes and mortality²⁶. Plaque morphology analysis showed a trend suggestive of unstable and vulnerable plaque characteristics in diabetics vs. non-diabetics (lipid volume index x μm 947 vs. 762; cap thickness μm 96 vs. 104) although this did not reach statistical significance. However, there was a significantly decreased calcium volume in these patients (2.7 vs. 4.2 mm^3 ; $p=0.01$). Hence, we hypothesise that diabetes was related to small calcifications with a spotty distribution pattern and thin fibrous cap with increased lipid core as seen in the culprit lesions of patients with acute coronary syndrome rendering the plaque unstable^{27,28}. This is similar to findings from an institutional OCT imaging registry-based analysis of spotty calcification and plaque vulnerability in patients with stable CAD in which, however, total calcium volume was not assessed¹⁰.

Our data also suggest that increase in calcium volume was not only associated with decreased plaque lipid burden but also an increase in fibrous cap thickness, although the latter finding was observed only in unadjusted analyses. This is similar to findings from other studies which showed that calcified plaques are more quiescent and passive compared to plaques with increased lipid burden and are more likely to be present in patients with stable CAD²⁹. Also, in another IVUS-based intracoronary calcium analysis using calcium arc area in patients with stable CAD and acute coronary syndrome, culprit lesions of patients with stable angina

pectoris had the highest calcium volume compared to unstable angina and acute myocardial infarction⁹. Hence, increased calcification within the plaque could lead to a decrease in mechanical stress and increase in plaque stability, thus making it less vulnerable⁷.

Limitations

An important limitation of this study is its retrospective nature. Thus, our results cannot be interpolated to assess the causal temporal relationship between CAC and lipid volume in patients with stable CAD. Also, there are no follow-up clinical data available at this time to translate these findings into any clinical outcome difference in patients with different calcium volume. Finally, there could be selection and collider-stratification bias as the OCT was performed based on the operator's discretion.

Conclusions

In patients with stable CAD, culprit lesions with increased coronary calcification by OCT are characterised by reduced plaque lipid content. Plaque cap thickness increased with increase in calcium volume. Further ongoing studies linked with clinical outcomes are essential to understand the implications of our findings from this study better.

Impact on daily practice

This study demonstrates a paradoxical relationship between CAC volume and lipid content independent of statin use which is important as current medical therapy is directed by total calcium burden. This study also demonstrates a similar inverse relationship between LDL cholesterol and CAC independent of statin use. Increase in calcification was associated with denser plaque (increase in atheroma cap thickness) resulting in plaque stability, although this association became insignificant after adjusting for other confounding factors.

Conflict of interest statement

The authors have no conflicts of interest to declare.

References

1. Vedanthan R, Seligman B, Fuster V. Global perspective on acute coronary syndrome: a burden on the young and poor. *Circ Res*. 2014;114:1959-75.
2. Crea F, Liuzzo G. Pathogenesis of acute coronary syndromes. *J Am Coll Cardiol*. 2013;61:1-11.
3. Falk E. Morphologic features of unstable atherothrombotic plaques underlying acute coronary syndromes. *Am J Cardiol*. 1989; 63:114E-120E.
4. Bentzon JF, Otsuka F, Virmani R, Falk E. Mechanisms of plaque formation and rupture. *Circ Res*. 2014;114:1852-66.
5. Criqui MH, Denenberg JO, Ix JH, McClelland RL, Wassel CL, Rifkin DE, Carr JJ, Budoff MJ, Allison MA. Calcium density of coronary artery plaque and risk of incident cardiovascular events. *JAMA*. 2014;311:271-8.
6. Shaw LJ, Narula J, Chandrashekhara Y. The never-ending story on coronary calcium. Is it predictive, punitive or protective? *J Am Coll Cardiol*. 2015;65:1283-5.
7. Huang H, Virmani R, Younis H, Burke AP, Kamm RD, Lee RT. The impact of calcification on the biomechanical stability of atherosclerotic plaques. *Circulation*. 2001;103:1051-6.
8. Dargas GD, Maehara A, Evrard SM, Sartori S, Li JR, Chirumamilla AP, Nomura-Kitabayashi A, Gukathasan N, Hassanin A, Baber U, Fahy M, Fuster V, Mintz GS, Kovacic JC. Coronary artery calcification is inversely related to body morphology in patients with significant coronary artery disease: a three-dimensional intravascular ultrasound study. *Eur Heart J Cardiovasc Imaging*. 2014;15:201-9.
9. Wang X, Lu C, Chen X, Zhao X, Xia D. A new method to quantify coronary calcification by intravascular ultrasound - the different patterns of acute myocardial infarction, unstable angina pectoris and stable angina pectoris. *J Invasive Cardiol*. 2008; 20:587-90.
10. Kataoka Y, Puri R, Hammadah M, Duggal B, Uno K, Kapadia SR, Tuzcu EM, Nissen SE, Nicholls SJ. Spotty calcification and plaque vulnerability in vivo: frequency-domain optical coherence tomography analysis. *Cardiovasc Diagn Ther*. 2014; 4:460-9.
11. Tearney GJ, Regar E, Akasaka T, Adriaenssens T, Barlis P, Bezerra HG, Bouma B, Bruining N, Cho JM, Chowdhary S, Costa MA, de Silva R, Dijkstra J, Di Mario C, Dudek D, Falk E, Feldman MD, Fitzgerald P, Garcia-Garcia HM, Gonzalo N, Granada JF, Guagliumi G, Holm NR, Honda Y, Ikeno F, Kawasaki M, Kochman J, Koltowski L, Kubo T, Kume T, Kyono H, Lam CC, Lamouche G, Lee DP, Leon MB, Maehara A, Manfrini O, Mintz GS, Mizuno K, Morel MA, Nadkarni S, Okura H, Otake H, Pietrasik A, Prati F, Räber L, Radu MD, Rieber J, Riga M, Rollins A, Rosenberg M, Sirbu V, Serruys PW, Shimada K, Shinke T, Shite J, Siegel E, Sonoda S, Suter M, Takarada S, Tanaka A, Terashima M, Thim T, Uemura S, Ughi GJ, van Beusekom HM, van der Steen AF, van Es GA, van Soest G, Virmani R, Waxman S, Weissman NJ, Weisz G; International Working Group for Intravascular Optical Coherence Tomography (IWG-IVOCT). Consensus standards for acquisition, measurement, and reporting of intravascular optical coherence tomography studies: a report from the International Working Group for Intravascular Optical Coherence Tomography Standardization and Validation. *J Am Coll Cardiol*. 2012;59:1058-72.
12. Dohi T, Maehara A, Moreno PR, Baber U, Kovacic JC, Limaye AM, Ali ZA, Sweeny JM, Mehran R, Dargas GD, Xu K, Sharma SK, Mintz GS, Kini AS. The relationship among extent of lipid-rich plaque, lesion characteristics, and plaque progression/regression in patients with coronary artery disease: a serial near-infrared spectroscopy and intravascular ultrasound study. *Eur Heart J Cardiovasc Imaging*. 2015;16:81-7.
13. Roleder T, Kovacic JC, Ali Z, Sharma R, Cristea E, Moreno P, Sharma SK, Narula J, Kini AS. Combined NIRS and IVUS imaging detects vulnerable plaque using a single catheter system: a head-to-head comparison with OCT. *EuroIntervention*. 2014;10:303-11.

14. Kato K, Yonetsu T, Kim SJ, Xing L, Lee H, McNulty I, Yeh RW, Sakhuja R, Zhang S, Uemura S, Yu B, Mizuno K, Jang IK. Nonculprit plaques in patients with acute coronary syndromes have more vulnerable features compared with those with non-acute coronary syndromes: a 3-vessel optical coherence tomography study. *Circ Cardiovasc Imaging*. 2012;5:433-40.
15. Prati F, Regar E, Mintz GS, Arbustini E, Di Mario C, Jang IK, Akasaka T, Costa M, Guagliumi G, Grube E, Ozaki Y, Pinto F, Serruys PW; Expert's OCT Review Document. Expert review document on methodology, terminology, and clinical applications of optical coherence tomography: physical principles, methodology of image acquisition, and clinical application for assessment of coronary arteries and atherosclerosis. *Eur Heart J*. 2010;31:401-15.
16. Kume T, Okura H, Kawamoto T, Yamada R, Miyamoto Y, Hayashida A, Watanabe N, Neishi Y, Sadahira Y, Akasaka T, Yoshida K. Assessment of the coronary calcification by optical coherence tomography. *EuroIntervention*. 2011;6:768-72.
17. Mehanna E, Bezerra HG, Prabhu D, Brandt E, Chamié D, Yamamoto H, Attizzani GF, Tahara S, Van Ditzhuijzen N, Fujino Y, Kanaya T, Stefano G, Wang W, Gargasha M, Wilson D, Costa MA. Volumetric characterization of human coronary calcification by frequency-domain optical coherence tomography. *Circ J*. 2013;77:2334-40.
18. Mintz GS, Nissen SE, Anderson WD, Bailey SR, Erbel R, Fitzgerald PJ, Pinto FJ, Rosenfield K, Siegel RJ, Tuzcu EM, Yock PG. American College of Cardiology Clinical Expert Consensus Document on Standards for Acquisition, Measurement and Reporting of Intravascular Ultrasound Studies (IVUS). A report of the American College of Cardiology Task Force on Clinical Expert Consensus Documents. *J Am Coll Cardiol*. 2001;37:1478-92.
19. Bland JM, Altman DG. Statistical methods for assessing agreement between two methods of clinical measurement. *Lancet*. 1986;1:307-10.
20. Kim SJ, Lee H, Kato K, Yonetsu T, Xing L, Zhang S, Jang IK. Reproducibility of in vivo measurements for fibrous cap thickness and lipid arc by OCT. *JACC Cardiovasc Imaging*. 2012;5:1072-4.
21. Terry JG, Carr JJ, Kouba EO, Davis DH, Menon L, Bender K, Chandler ET, Morgan T, Crouse JR 3rd. Effect of simvastatin (80 mg) on coronary and abdominal aortic arterial calcium (from the coronary artery calcification treatment with zocor [CATZ] study). *Am J Cardiol*. 2007;99:1714-7.
22. Puri R, Nicholls SJ, Shao M, Kataoka Y, Uno K, Kapadia SR, Tuzcu EM, Nissen SE. Impact of statins on serial coronary calcification during atheroma progression and regression. *J Am Coll Cardiol*. 2015;65:1273-82.
23. Budoff MJ, Lane KL, Bakhsheshi H, Mao S, Grassmann BO, Friedman BC, Brundage BH. Rates of progression of coronary calcium by electron beam tomography. *Am J Cardiol*. 2000;86:8-11.
24. Henein MY, Owen A. Statins moderate coronary stenoses but not coronary calcification: results from meta-analyses. *Int J Cardiol*. 2011;153:31-5.
25. Wong ND, Nelson JC, Granston T, Bertoni AG, Blumenthal RS, Carr JJ, Guerci A, Jacobs DR Jr, Kronmal R, Liu K, Saad M, Selvin E, Tracy R, Detrano R. Metabolic syndrome, diabetes, and incidence and progression of coronary calcium: the Multiethnic Study of Atherosclerosis study. *JACC Cardiovasc Imaging*. 2012;5:358-66.
26. Agarwal S, Cox AJ, Herrington DM, Jorgensen NW, Xu J, Freedman BI, Carr JJ, Bowden DW. Coronary calcium score predicts cardiovascular mortality in diabetes: diabetes heart study. *Diabetes Care*. 2013;36:972-7.
27. Ehara S, Kobayashi Y, Yoshiyama M, Shimada K, Shimada Y, Fukuda D, Nakamura Y, Yamashita H, Yamagishi H, Takeuchi K, Naruko T, Haze K, Becker AE, Yoshikawa J, Ueda M. Spotty calcification typifies the culprit plaque in patients with acute myocardial infarction: an intravascular ultrasound study. *Circulation*. 2004;110:3424-9.
28. Motoyama S, Kondo T, Sarai M, Sugiura A, Harigaya H, Sato T, Inoue K, Okumura M, Ishii J, Anno H, Virmani R, Ozaki Y, Hishida H, Narula J. Multislice computed tomographic characteristics of coronary lesions in acute coronary syndromes. *J Am Coll Cardiol*. 2007;50:319-26.
29. New SE, Aikawa E. Molecular imaging insights into early inflammatory stages of arterial and aortic valve calcification. *Circ Res*. 2011;108:1381-91.

Supplementary data

Online Table 1. Baseline angiographic and procedural characteristics.

Online Table 2. Multivariable adjusted linear regression of clinical and OCT characteristics with total calcium volume.

Online Table 3. Multivariable adjusted logistic regression of clinical and OCT characteristics with total calcium volume as binary variable.

Online Figure 1. Bland-Altman analysis of calcium volume (mm³) by two independent observers.

Online Figure 2. Bland-Altman plots of mean calcium arc by IVUS and OCT imaging.

Online Figure 3. Bland-Altman plots of mean calcium length by IVUS and OCT imaging.

Online Figure 4A. Calcification identified by QCA vs. OCT.

Online Figure 4B. Calcification identified by QCA by OCT calcium volume (mm³).

The supplementary data are published online at:

http://www.pcronline.com/eurointervention/118th_issue/48



Supplementary data

Online Table 1. Baseline angiographic and procedural characteristics.

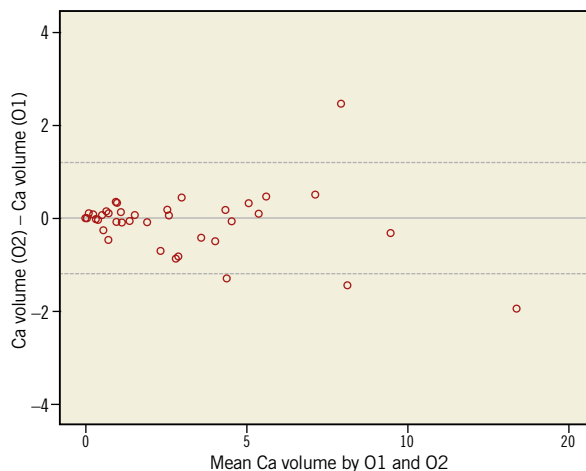
Variable*		Total N=250	Ca group 1 N=84	Ca group 2 N=83	Ca group 3 N=83	p-value†
Quantitative coronary angiography						
Lesion location	Left anterior descending	135 (54)	52 (62)	33 (40)	50 (60)	0.07
	Left circumflex	54 (22)	15 (18)	23 (28)	16 (19)	
	Right coronary artery	60 (24)	17 (20)	26 (31)	17 (21)	
	Saphenous vein graft	1 (0.4)	0	1 (1.2)	0	
Preprocedural measurements	Reference vessel diameter, mm	2.7±0.5	2.6±0.5	2.78±0.5	2.7±0.4	0.06
	Minimal lumen diameter, mm	1.27±0.4	1.27±0.4	1.29±0.4	1.26±0.42	0.87
	Diameter stenosis, %	52.1±14.8	50.2±15.7	53.1±13	52.9±15.7	0.28
	Lesion length, mm	16.5±8.2	15.3±8.8	17.9±8.3	16.3±7.2	0.03
Calcification evaluated by angiography	None or mild	177 (71)	80 (95)	64 (77)	33 (40)	<0.001
	Moderate	65 (26)	4 (5)	19 (23)	42 (51)	
	Severe	8 (3.2)	0	0	8 (9.6)	
	Eccentric lesion**	39 (15.6)	15 (17.9)	12 (14.5)	12 (14.5)	
Optical coherence tomography (OCT)						
Calcium volume measured, mm ³	Mean±SD	3.4±5.75	0.02±0.04	1.3±0.82	9.08±7.14	0.0001
	Median	1.02	0	1.03	7.23	–
	Interquartile range	0-4.13	0-0	0.63-1.99	4.2-11.8	–
	Minimum value	0	0	0.23	3.1	0.0001
	Maximum value	45.4	0.20	3.01	45.4	0.0001
* Mean±SD for normally distributed continuous variables and median (IQR) for non-parametric variables; categorical variables expressed as n (%). **Edge in the outer ¼ of the apparently normal lumen. † ANOVA for normally distributed continuous variables and Kruskal-Wallis test for non-parametric variables; chi-square test for categorical variables.						

Online Table 2. Multivariable adjusted linear regression of clinical and OCT characteristics with total calcium volume.

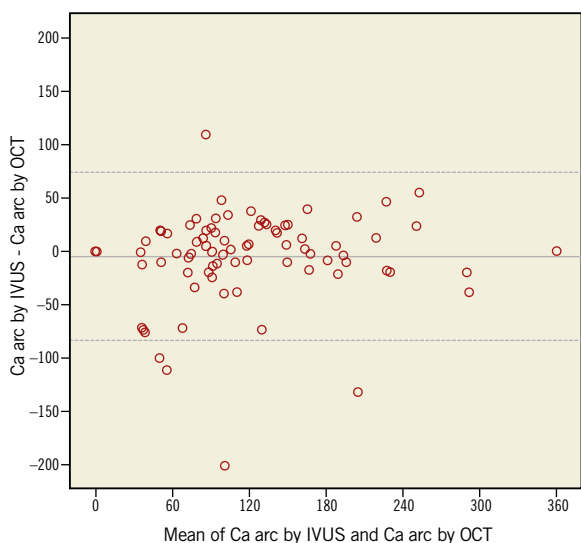
Variable*	Partial regression coefficient	p-value
Age	0.02 (–0.06 to 0.10)	0.65
Male gender	1.88 (–0.12 to 3.89)	0.06
Diabetes	–0.94 (–2.58 to 0.70)	0.26
Prior MI	4.1 (1.55–6.54)	0.02
LDL cholesterol	–0.06 (–0.13 to 0.01)	0.08
Lipid volume index	–0.002 (–0.003 to 0.0001)	0.05
Average lipid arc	0.001 (–0.01 to 0.023)	0.26
Minimum cap thickness	0.01 (–0.01 to 0.03)	0.16
*Model adjusted for all clinical and OCT factors that predicted calcium volume in unadjusted linear regression. LDL: low-density lipoprotein; MI: myocardial infarction		

Online Table 3. Multivariable adjusted logistic regression of clinical and OCT characteristics with total calcium volume as binary variable.

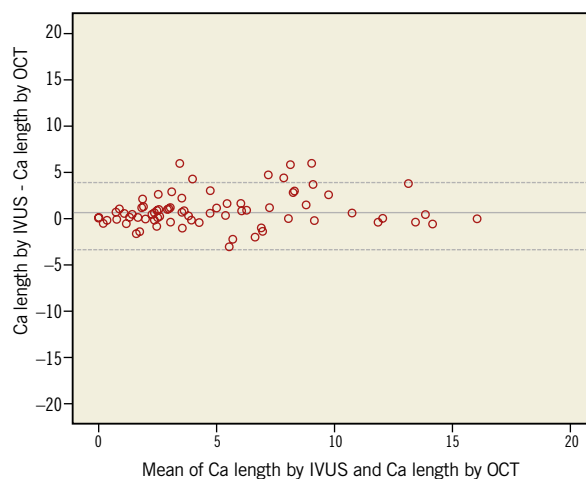
Variable*	Odds ratio	p-value
Age	1.02 (0.99-1.05)	0.21
Male gender	2.10 (1.06-4.11)	0.03
Diabetes	0.51 (0.27-0.97)	0.04
Prior MI	1.23 (0.44-3.46)	0.68
LDL cholesterol	1.00 (0.99-1.01)	0.92
Lipid length	0.92 (0.85-0.99)	0.03
Average lipid arc	0.99 (0.99-1.01)	0.91
Minimum cap thickness	0.99 (0.98-1.01)	0.25
*Model adjusted for all clinical and OCT factors that predicted calcium volume in unadjusted analysis. LDL: low-density lipoprotein; MI: myocardial infarction; OCT: optical coherence tomography		



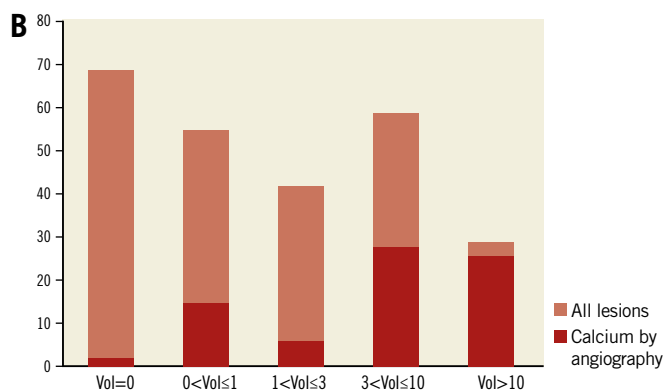
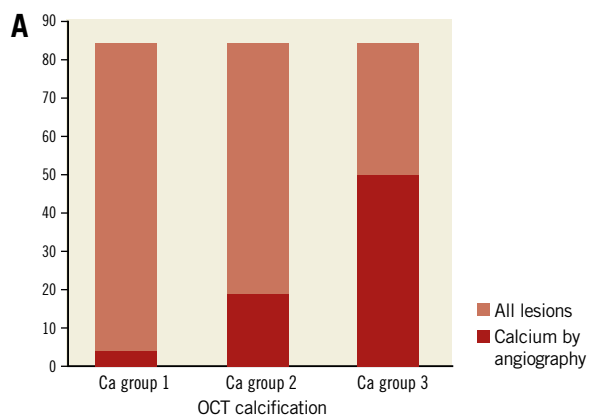
Online Figure 1. Bland-Altman analysis of calcium volume (mm^3) by two independent observers.



Online Figure 2. Bland-Altman plots of mean calcium arc by IVUS and OCT imaging. Middle line corresponds to the mean difference; dotted lines represent $\pm 1.96 \times \text{SD}$. IVUS: intravascular ultrasound; OCT: optical coherence tomography



Online Figure 3. Bland-Altman plots of mean calcium length by IVUS and OCT imaging. Middle line corresponds to the mean difference; dotted lines represent $\pm 1.96 \times \text{SD}$. IVUS: intravascular ultrasound; OCT: optical coherence tomography



Online Figure 4. Calcification. A) Calcification identified by QCA vs. OCT. OCT calcification: Ca group 1 Ca group 2 Ca group 3. B) Calcification identified by QCA by OCT calcium volume (mm^3). OCT: optical coherence tomography; QCA: quantitative coronary angiography